New transgenic mouse lines for selectively targeting astrocytes and for studying calcium signals in astrocyte processes *in situ* and *in vivo*

[1]Rahul Srinivasan*, [1]Tsai-Yi Lu*, [1]Hua Chai*, [1]Ji Xu, [3]Ben Huang, [3,6,7]Peyman Golshani, [3,4,5]Giovanni Coppola & [1,2]Baljit S. Khakh*,Ψ

Departments of [1]Physiology, [2]Neurobiology, [3]Neurology, [4]Psychiatry and Biobehavioral Sciences, [5]Center for Neurobehavioral Genetics, Semel Institute for Neuroscience and Human Behavior, [6]Integrative Center for Learning and Memory, David Geffen School of Medicine, University of California Los Angeles, Los Angeles USA CA 90095-1751. [7]West Los Angeles VA Medical Center, Los Angeles, CA 90073

* Co-first authors (RS, T-YL, HC)

Supplemental Information

1. Supplemental Movie 1
2. Seven Supplemental figures and legends
3. Supplemental Tables 1-3 and legends
4. Detailed methods
5. Supplemental Excel file (attached separately)
   - Table 1: Raw FPKM values for input and IP for all 4 replicates
   - Table 2: Astrocyte enriched genes by percentile
   - Table 3: Top differentially expressed genes between P7 and P30
   - Table 4: ENRICHR Gene Ontology analysis for top differentially expressed genes between P7 and P30

6. Raw and normalized RNAseq data have been deposited in the Gene Expression Omnibus repository (http://www.ncbi.nlm.nih.gov/geo) with accession number GSE84540.

Supplemental movie S1: related to Figure 2. GCaMP6f expression in example brain areas of a representative sagittal brain section resulting from tamoxifen induced gene expression in mice that were made by crossing *Aldh1l1*-Cre/ERT2 and Ai95 mice. Average data are reported in the main text.

Supplemental Excel file Table 1: related to Figure 7. Raw FPKM values for input and IP for all 4 replicates from the cortical RNAseq data.

Supplemental Excel file Table 2: related to Figure 7. Astrocyte enriched genes by percentile (from the cortical RNAseq data).

Supplemental Excel file Table 3: related to Figure 7. Top differentially expressed genes between P7 and P30 for cortical astrocytes (from the RNAseq data).

Supplemental Excel file Table 4: related to Figure 7. ENRICHR Gene Ontology analysis for top differentially expressed genes between P7 and P30 for cortical astrocytes (from the RNAseq data).
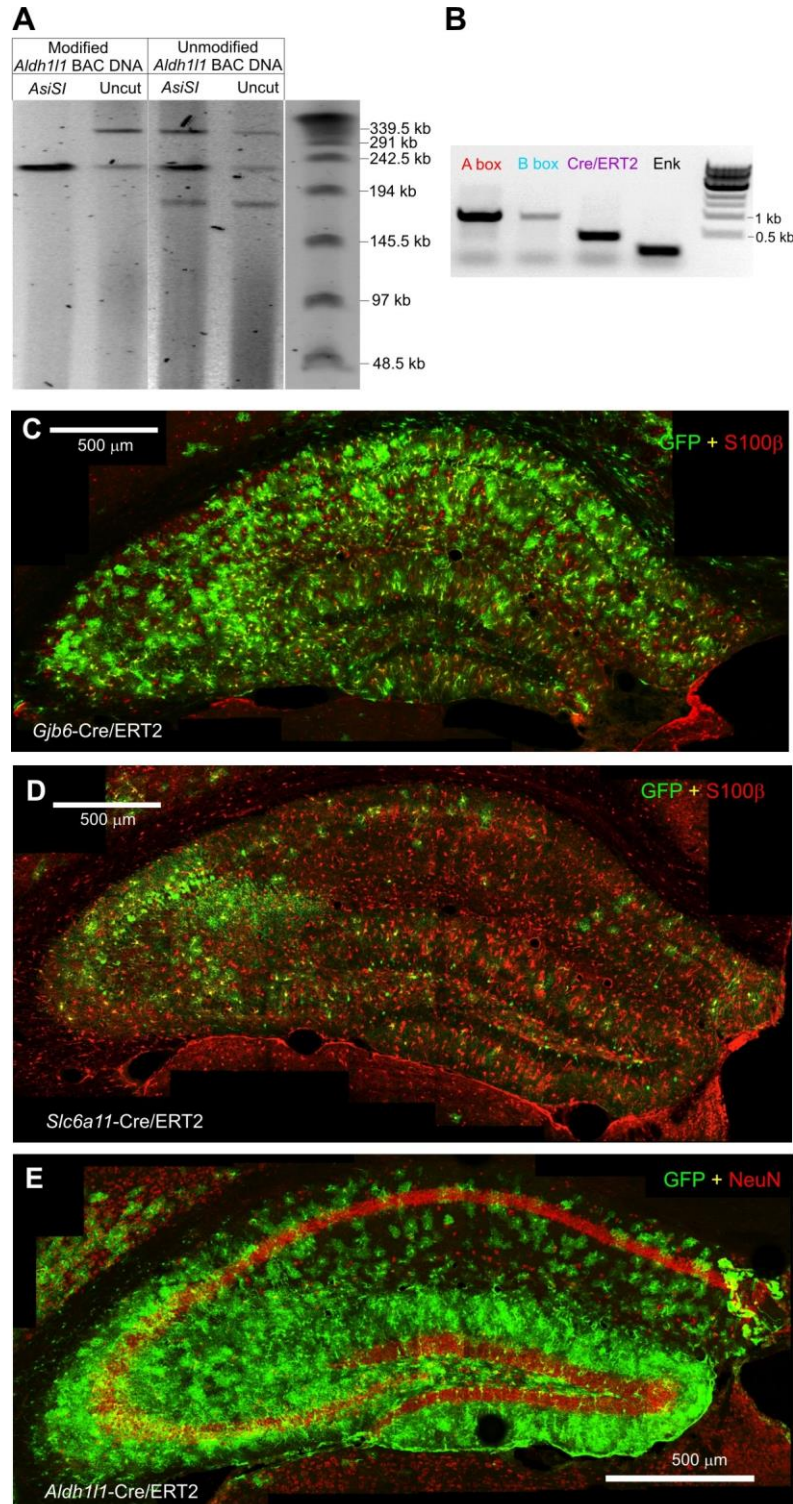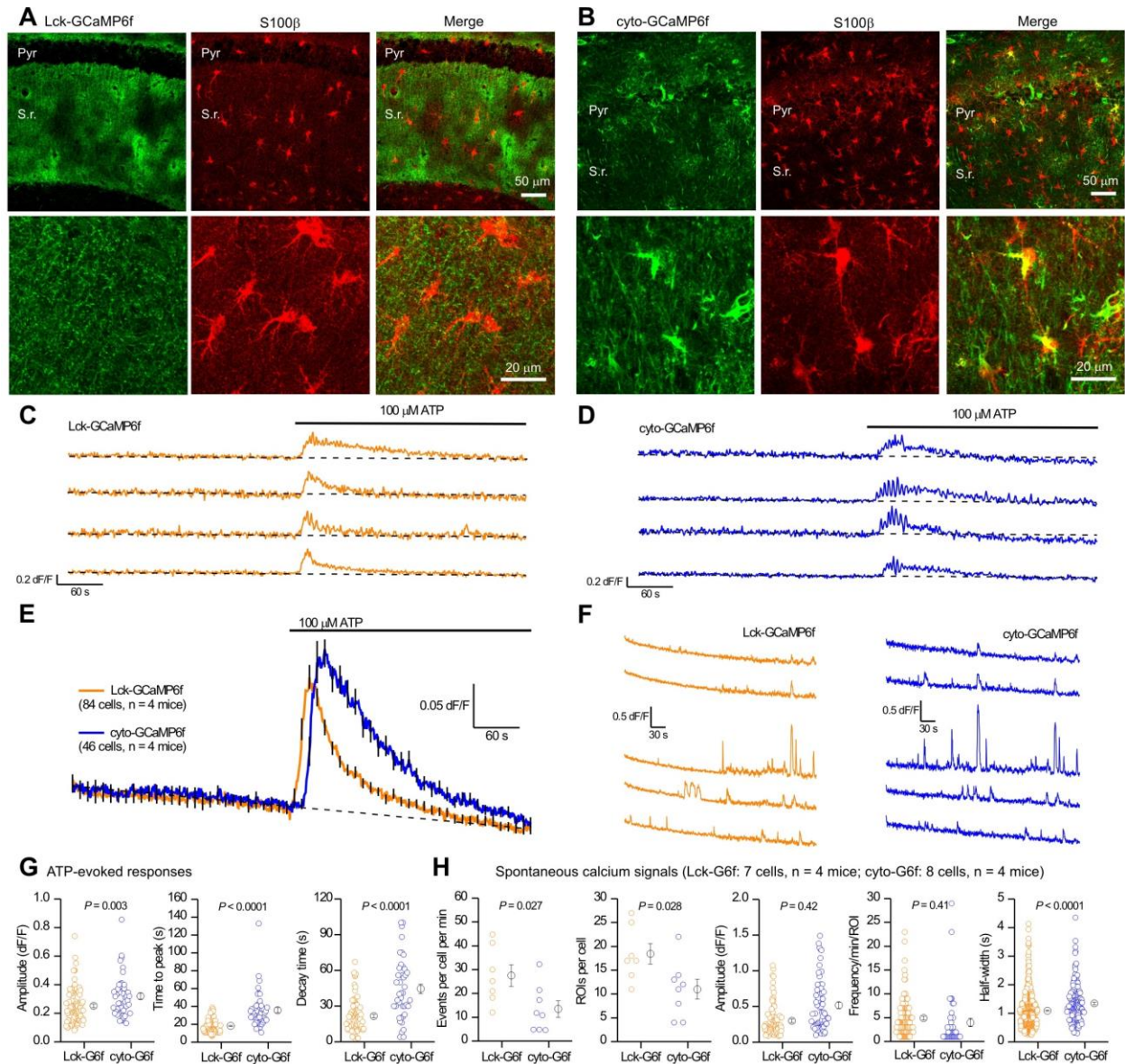
Supplemental Figure 1: Related to Figure 1. Construction of *Aldh1l1*-Cre/ERT2 transgenic mice and characterization of *Gjb6*-Cre/ERT2, *Slc6a11*-Cre/ERT2 and *Aldh1l1*-Cre/ERT2 BAC transgenic mice using AAV FLEX-GFP virus. A. Pulse field gel electrophoresis of modified and unmodified *Aldh1ll* BAC DNA cut with *AsiS1*. *AsiS1* linearizes the modified *Aldh1l1*-Cre/ERT2 BAC, but fails to cut the unmodified *Aldh1l1* BAC. **B.** Genotyping of the *Aldh1l1*-Cre/ERT2 BAC transgenic mouse with primers flanking the A box, B box, and Cre/ERT2 cassette (see Figure 1A of main text). Proenkephalin (Enk) primers were used as a positive control. **C.** Representative hippocampal montage of the *Gjb6*-Cre/ERT2 transgenic mouse stained for GFP (green) and S100β (red) after injection with AAV FLEX GFP and tamoxifen (75 mg/kg i.p for 5 consecutive days) shows expression of GFP in astrocytes as well as neurons. **D. As in C,** but for a *Slc6a11*-Cre/ERT2 BAC transgenic mouse. **E.** Representative hippocampal montage of the *Aldh1l1*-Cre/ERT2 transgenic mouse stained for GFP (green) and NeuN (red) after injection with AAV FLEX GCaMP6f (immunostained with GFP antibodies) and tamoxifen (75 mg/kg i.p for 5 consecutive days) shows expression of GFP in astrocytes, but not in neurons.
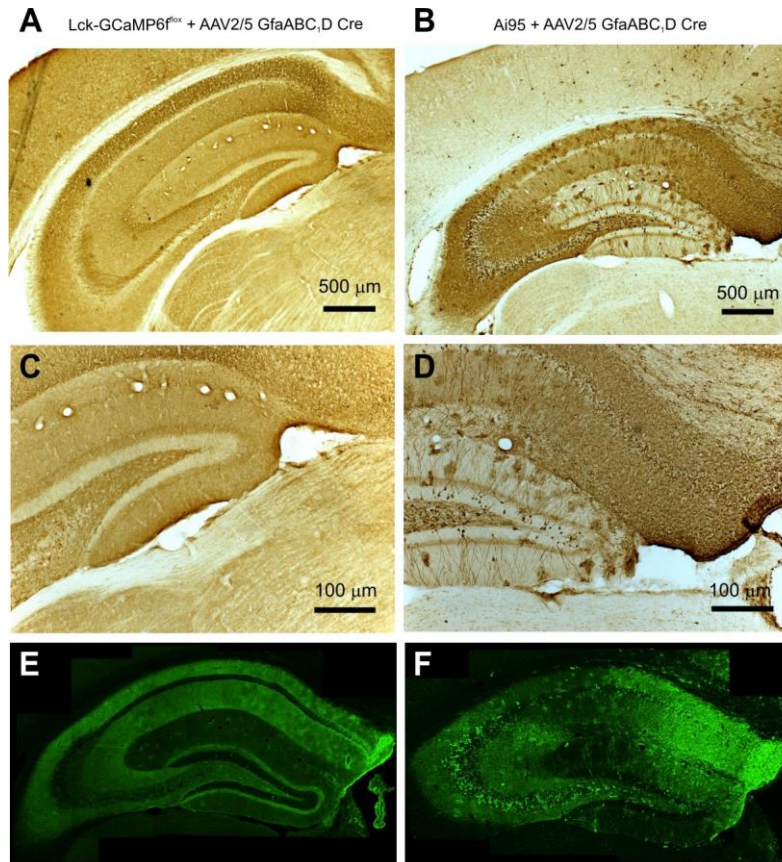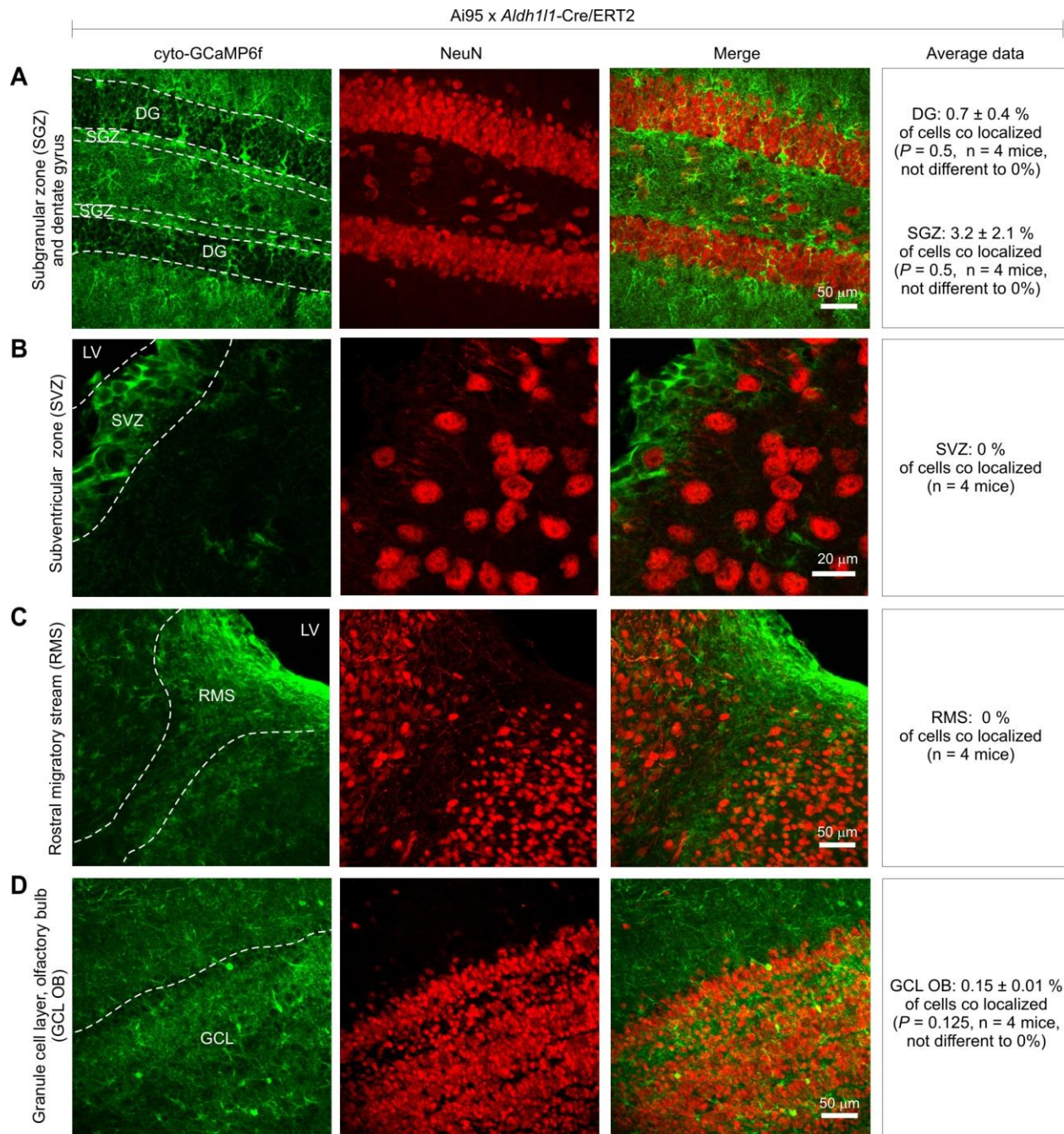
Supplemental Figure 2: Related to figure 2. DAB and fluorescence staining of Lck-GCaMP6f^{flox} and Ai95 mice injected with AAV2/5 GfaABC$_1$D Cre virus. A. DAB stained hippocampus from Lck-GCaMP6f^{flox} mouse injected with AAV2/5 GfaABC$_1$D Cre virus shows a uniform brown staining throughout the hippocampus. **B.** DAB stained hippocampus from Ai95 mouse injected with AAV2/5 GfaABC$_1$D Cre virus shows dark brown staining of astrocytes and neurons throughout the hippocampus. **C.** High magnification image of DAB stained hippocampus shown in A. **D.** High magnification image of DAB stained hippocampus shown in **B**. **E.** Representative montage of hippocampus from the Lck-GCaMP6f^{flox} mouse injected with AAV2/5 GfaABC$_1$D Cre virus and stained with GFP antibody shows a uniform expression of Lck-GCaMP6f in the neuropil of the hippocampus. **F.** Representative montage of hippocampus from the Lck-GCaMP6f^{flox} mouse injected with AAV2/5 GfaABC$_1$D Cre virus and stained with GFP antibody shows expression of cyto-GCaMP6f in the neuronal and astrocytic cell bodies throughout the hippocampus.
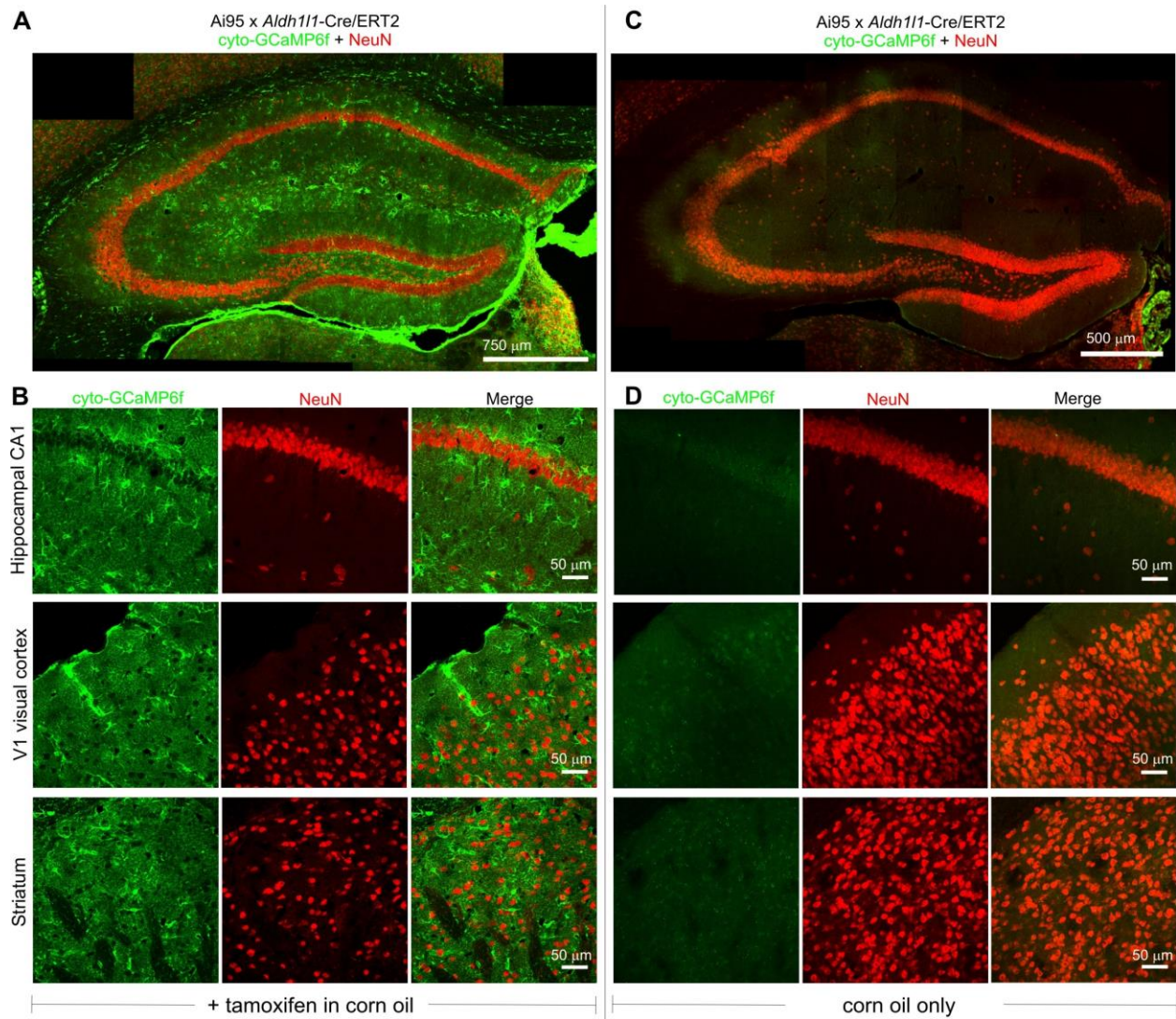
Supplemental Figure 3: Related to figure 3. Functional characterization of the Lck-GCaMP6f$^{\text{flox}}$ knock-in mice. A. Representative image of the hippocampal CA1 region from Lck-GCaMP6f$^{\text{flox}}$ knock-in mice injected with AAV2/5 GfaABC$_1$D Cre, stained for Lck-GCaMP6f (green) and S100β (red). Pyr is the pyramidal cell layer and S.r is the Stratum radiatum. Lower panels are high magnification images of the CA1 Stratum radiatum. **B.** As in A, but for Ai95 mice. **C.** Representative responses of Lck-GCaMP6f$^{\text{flox}}$ knock-in mice injected with AAV2/5 GfaABC$_1$D Cre virus to bath application of 100 μM ATP. **D.** Representative responses of Ai95 mice injected with AAV2/5 GfaABC$_1$D Cre virus to bath application of 100 μM ATP. **E.** Average traces for experiments such as those in **C-D**. **F.** Representative traces of spontaneous calcium signals from the processes of astrocytes in the Lck-GCaMP6f$^{\text{flox}}$ and Ai95 mice injected with AAV2/5 GfaABC$_1$D Cre virus. **G.** Scatter plots of ATP-evoked responses in Lck-GCaMP6f$^{\text{flox}}$ knock-in mice. **H.** Scatter plots for spontaneous calcium signals events in the Lck-GCaMP6f$^{\text{flox}}$ knock-in and Ai95 mice.
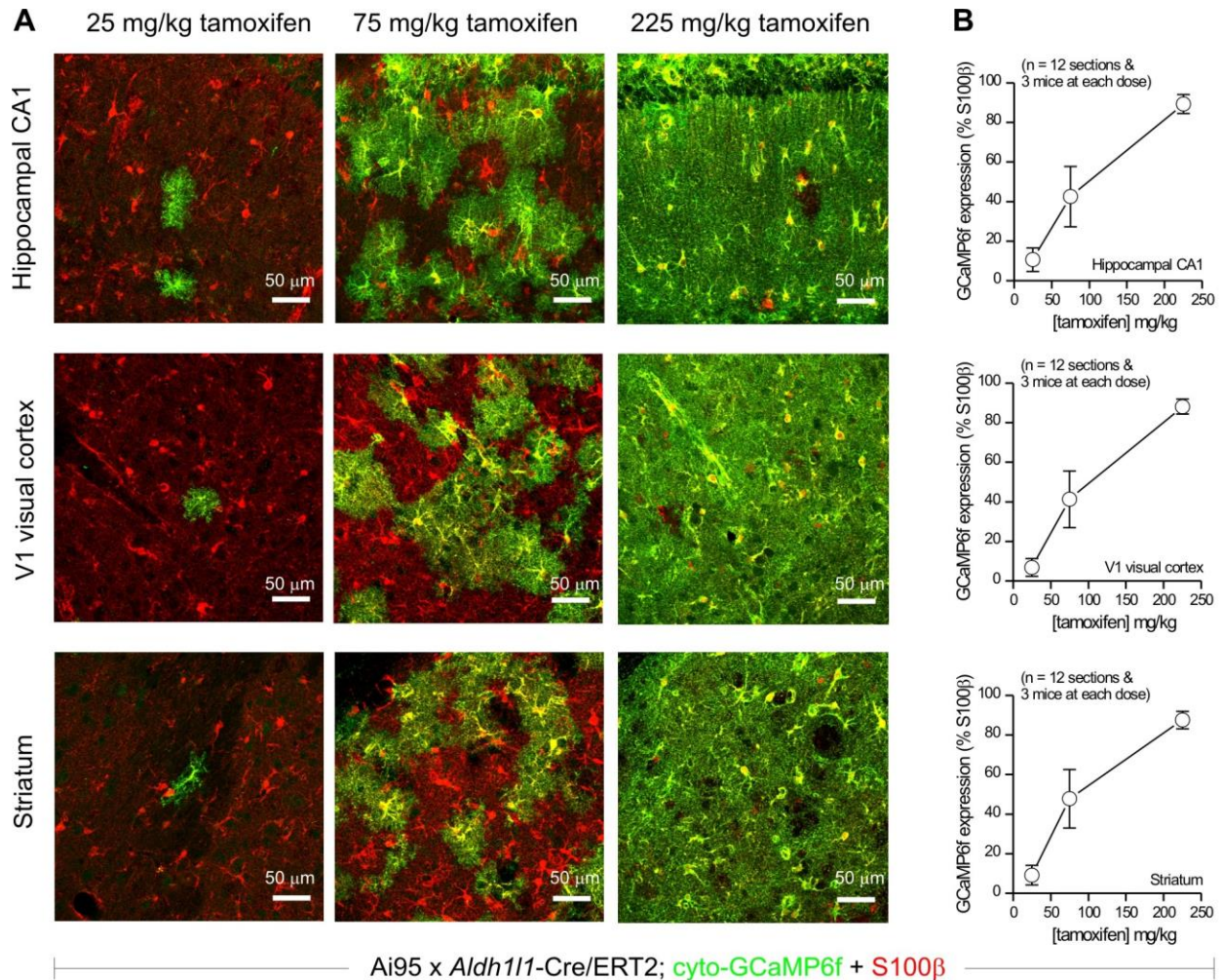
Supplemental Figure 4: Related to figure 3. No expression of cyto-GCaMP6f in NeuN positive cells when driven by *Aldh1l1*-Cre/ERT2 in Ai95 mice at ~P80. The representative images show no colocalisation between cyto-GCaMP6f and NeuN in the subgranular zone (**A**), the subventricular zone (**B**), the rostral migratory stream (**C**) or the granule cell later of the olfactory bulb (**D**). Although a few neurons in the dentate gyrus (0.7%) and olfactory bulb granule cell layer (0.15%) seemingly colocalized with NeuN, the average data were not statistically significant from 0% co labelling (n = 4 mice in each case). Thus, the possibility of significant neuronal expression of reporters with the *Aldh1l1*-Cre/ERT2 mice under the conditions we have examined is extremely low. Additional issues are discussed in the main text.

Supplemental Figure 5: related to figures 2 and 3. No expression of cyto-GCaMP6f in the absence of tamoxifen when driven by *Aldh1l1*-Cre/ERT2 in Ai95 mice at ~P80. A-B. Tamoxifen driven cyto-GCaMP6f expression in the hippocampus (**A**). Higher magnification areas of the hippocampal CA1 region, V1 visual cortex and dorsolateral striatum (**B**) are also shown. **C-D.** As in A-B, but when no tamoxifen was administered (corn oil was administered instead). There was no detectable cyto-GCaMP6f expression anywhere. The green haze is auto fluorescence. The images are shown with the exact same laser power, acquisition settings and gray scale pixel values. Each image is representative of 4 mice.

Supplemental Figure 6: related to figures 2 and 3. Cyto-GCaMP6f expression when driven by *Aldh1l1*-Cre/ERT2 in Ai95 mice at ~P66 was dependent on the tamoxifen dose administered *in vivo*. A. Representative images showing cyto-GCaMP6f expression as a function of tamoxifen dose in hippocampal CA1, V1 visual cortex and striatal brain sections. **B.** Average data showing the % of S100β positive cells that expressed cyto-GCaMP6f in the three brain areas as a function of tamoxifen dose. In all three brain areas, cyto-GCaMP6f expression was dependent on the tamoxifen dose, but there were no detectable differences between these areas.

Additional note: In our standard protocol (Madisen et al., 2010) that we used throughout this study, we administered tamoxifen at 75 mg/kg once per day for five days and assessed gene expression 14-21 days later at ~P80. However, since tamoxifen may accumulate in body compartments over multiple days this protocol cannot be used to reliably assess the tamoxifen dose dependence of gene expression. In order to assess this aspect, we administered tamoxifen only once at 25, 75 and 225 mg/kg (at P56) and assessed gene expression 10 days later, as previously described (Chow et al., 2008; Nakamura et al., 2006). The results of these experiments are reported in this figure.
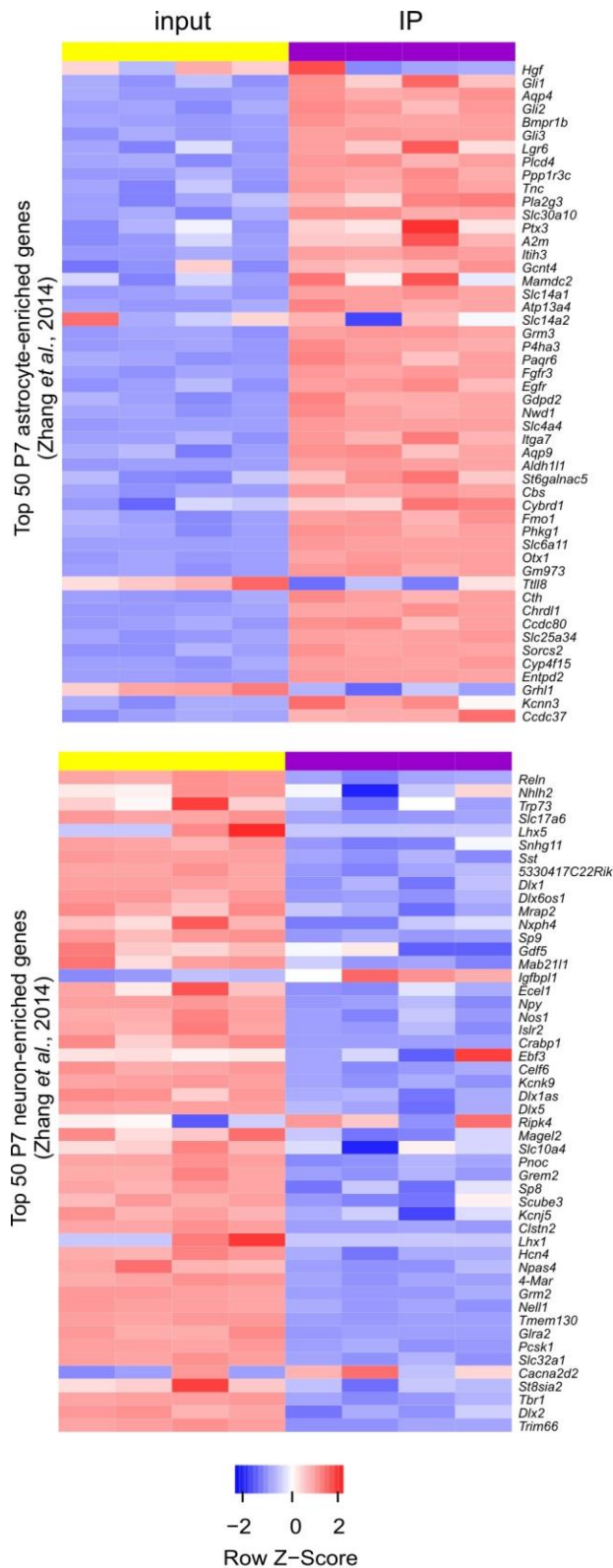
Supplemental Figure 7: related to figure 7. Validation of the P80 cortical astrocyte transcriptome.

Upper panel: a heat map showing relative expression (Row z-score) of the top 50 astrocyte genes from the P7 cortical RNAseq database in our P80 dataset. Row z-scores are shown as red for relative enrichment and as blue for relative depletion.

Lower panel: a heat map showing relative expression (Row z-score) of the top 50 neuronal genes from the P7 cortical RNAseq database in our P80 dataset. Row z-scores are shown as red for relative enrichment and as blue for relative depletion.

Note that overall, the top 50 astrocyte genes were enriched in our data set, whereas the top 50 neuronal genes were not. All the raw data are provided as part of **Supplementary Excel file 1 (Table 1)**. The data used for P7 were from Zhang *et al.,* (2014).

Supplemental Table 1: related to figure 7. Gene ontology analysis of astrocyte genes with differential expression (P7 v P80).

Gene ontology biological processes	# genes	q-value
behavior (GO:0007610)	9	5.70 E-07
organic anion transport (GO:0015711)	8	3.20 E-07
amino acid import (GO:0043090)	3	3.73 E-06
response to extracellular stimulus (GO:0009991)	7	3.45 E-06
cellular response to external stimulus (GO:0071496)	6	2.39 E-06
anion transport (GO:0006820)	8	2.93 E-06
response to drug (GO:0042493)	7	7.62 E-06
organic acid transport (GO:0015849)	6	7.34 E-06
carboxylic acid transport (GO:0046942)	6	6.99 E-06
cellular response to extracellular stimulus (GO:0031668)	5	5.43 E-06
amino acid transport (GO:0006865)	5	7.65 E-06
single-organism behavior (GO:0044708)	7	8.80 E-06
response to toxic substance (GO:0009636)	5	1.24 E-05
acidic amino acid transport (GO:0015800)	3	1.44 E-05
response to wounding (GO:0009611)	5	2.66 E-05
response to mechanical stimulus (GO:0009612)	5	3.4 E-05
regulation of neurotransmitter levels (GO:0001505)	4	4.22 E-05
learning or memory (GO:0007611)	5	5.87 E-05
regeneration (GO:0031099)	4	5.59 E-05
response to calcium ion (GO:0051592)	4	6.27 E-05
neurotransmitter transport (GO:0006836)	4	6.03 E-05
aging (GO:0007568)	5	6.74 E-05
cellular response to calcium ion (GO:0071277)	3	8.43 E-05
response to axon injury (GO:0048678)	3	9.06 E-05

     transport   response to stimulus   behavior

The top 25 biological process terms from gene ontology analysis for the 34 genes whose expression differed between cortical astrocyte enriched genes at P80 and P7 are listed (**Figure 7G**). The number of genes in each GO group and the q-value are reported. The complete list of GO groups with gene names are in the **Supplementary Excel file** (Table 4).

Supplemental Table 2: related to figure 7. 34 cortical astrocyte genes that were differentially expressed between P80 and P7.

Gene name	Zhang *et al.,* 2014		This study		
	P7 astrocyte FPKM	P7 percentile	P80 IP FPKM ± s.e.m.	P80 percentile	Δ percentile
Down at P80					
Fos	3527	1.0000	9.59 ± 3.55	0.0005	-0.9995
Fabp7	1604	0.4548	348 ± 70	0.0170	-0.4378
Cst3	3309	0.9383	10747 ± 972	0.5237	-0.4146
Jun	1164	0.3301	33.4 ± 10.3	0.0016	-0.3285
Ptprz1	1021	0.2895	59.7 ± 5.2	0.0029	-0.2866
Sparcl1	1768	0.5014	4453 ± 178	0.2170	-0.2844
Slc1a3	1144	0.3244	1009 ± 16	0.0492	-0.2753
Nr4a1	871	0.2469	15.5 ± 3.8	0.0008	-0.2461
Cyr61	842	0.2388	30.2 ± 6.1	0.0015	-0.2373
Ptn	914	0.2591	855 ± 31	0.0417	-0.2174
Bcan	818	0.2319	566 ± 15	0.0276	-0.2043
Hspa5	680	0.1929	145 ± 11	0.0071	-0.1858
Tspan7	1145	0.3246	2905 ± 90	0.1416	-0.1830
Mfge8	730	0.2071	606 ± 22	0.0295	-0.1775
Fosb	609	0.1728	0.55 ± 0.14	2.66 e-5	-0.1728
Psap	656	0.1860	292 ± 6	0.0142	-0.1718
Scd2	893	0.2531	1778 ± 88	0.0866	-0.1665
Ubc	579	0.1640	80.1 ± 3.1	0.0039	-0.1601
Slc1a2	732	0.2075	987 ± 27	0.0481	-0.1594
Slc6a11	564	0.1599	337 ± 6	0.0164	-0.1435
Malat1	515	0.1461	86.1 ± 22.6	0.0042	-0.1419
Atp1b2	624	0.1770	1066 ± 18	0.0519	-0.1251
Slc38a3	451	0.1279	85.0 ± 4.2	0.0041	-0.1238
Ppap2b	516	0.1464	562 ± 39	0.0274	-0.1191
Slco1c1	408	0.1158	63.0 ± 4.2	0.0031	-0.1127
Actg1	450	0.1275	320 ± 44	0.0156	-0.1119
Gja1	501	0.1420	628 ± 42	0.0306	-0.1114
Bhlhe40	392	0.1112	45.5 ± 3.3	0.0022	-0.1090
Slc6a1	425	0.1204	321 ± 12	0.0157	-0.1047
Up at P80					
Aldoc	512	0.1452	7378 ± 166	0.3596	0.2144
Glul	740	0.2097	7611 ± 508	0.3709	0.1612
Ckb	336	0.0953	5206 ± 333	0.2537	0.1584
Ptgds	1.7	0.0005	3086 ± 1205	0.0150	0.1499
Apoe	3006	0.8524	20520 ± 590	1.0000	0.1476

In this table, the FPKM values for the genes are taken from the **Supplementary Excel file** (Table 1) that is uploaded as part of this study at P80, or from Zhang *et al.,* 2014 for P7. The percentile FPKM in each dataset was determined relative to the highest expressed transcript in P80 IPs (*Apoe*) or in P7 astrocytes (*Fos*). The genes listed in the table are ordered according to magnitude of difference in percentile. Genes are color coded green for increased expression at P80 and red for decreased expression at P80.

Supplemental Table 3: related to figure 7. Representative astrocyte genes compared between P7 and P80.

Gene name	Common name	Zhang *et al.,* 2014		This study	
		P7 FPKM	P7 percentile	P80 FPKM ± s.e.m.	P80 percentile
Glul	Glutamine synthetase	740	0.21	7611 ± 508	0.37
Sparcl1	HEVIN	1768	0.50	4453 ± 178	0.22
Slc1a3	GLAST-1	1144	0.32	1009 ± 16	0.049
Slc1a2	Glt1	732	0.21	987 ± 27	0.048
S100b	S100β	31.2	0.088	933 ± 46	0.045
Gja1	Cx43	501	0.14	628 ± 42	0.031
Gfap	GFAP	127	0.036	548 ± 178	0.027
Kcnj10	Kir4.1	185	0.53	535 ± 27	0.026
Aldh1l1	Aldh1l1	145	0.041	406 ± 13	0.02
Sparc	SPARC/Osteonectin	111	0.032	228 ± 41	0.011
Grm3	mGluR3	158	0.045	114 ± 5	0.0056
Mertk	MERTK	33.8	0.0096	85.4 ± 6.6	0.0042
Slc17a7	vGlut1	0.51	N/E	26.1 ± 2.3	N/E
Megf10	MEGF10	25.2	0.0071	17.8 ± 1.0	0.00087
Thbs4	Thrombospondin 4	2.08	0.00059	6.27 ± 1.12	0.00031
Thbs3	Thrombospondin 3	4.78	N/E	2.72 ± 0.19	N/E
Slc32a1	vGat1	0.19	N/E	1.09 ± 0.16	N/E
Grm2	mGluR2	0.21	N/E	0.91 ± 0.07	N/E
Grm5	mGluR5	36.2	0.010	0.76 ± 0.11	0.000037
Slc18a2	vMat2	0.71	N/E	0.75 ± 0.18	N/E
Thbs2	Thrombospondin 2	1.11	N/E	0.65 ± 0.07	N/E
Slc17a6	vGlut2	0.13	N/E	0.16 ± 0.02	N/E
Thbs1	Thrombospondin 1	23.7	0.0067	0.16 ± 0.05	0.0000076
Slc17a9	vNut1	0.12	N/E	0.06 ± 0.04	N/E
Slc17a8	vGlut3	0.12	N/E	0.05 ± 0.01	N/E
Slc18a1	vMat1	≤ 0.1	N/E	0.02 ± 0.01	N/E
Slc18a3	vAChT	≤ 0.1	N/E	0.002 ± 0.002	N/E

Astrocyte markers Vesicular transporters Ion channels
Secreted factors Phagocytosis Receptors

In this table, the FPKM values for the representative genes are taken from the **Supplementary Excel file**, or from Zhang *et al.,* 2014 for P7. The log2(percentile FPKM) at both ages is shown for genes enriched in astrocyte at either P80 (2-fold over input) or at P7 (2-fold over average of all cell types; FPKM > 0.1). As a frame of reference, Log2(x) = y, then $x = 2^y$, where x is the percentile and y is the Log2 percentile. Also, the gene with the highest FPKM at P80 was *Apoe* with a value of 20520, and the gene with the highest FPKM at P7 was *Fos* with a value of 3527. Genes that were not enriched in astrocytes are denoted as "N/E".

Detailed experimental procedures

All animal experiments were conducted in accordance with the National Institute of Health Guide for the Care and Use of Laboratory Animals and were approved by the Chancellor's Animal Research Committee at the University of California, Los Angeles.

Adeno-associated viruses (AAVs)

In order to generate an AAV 2/5 capable of expressing Cre in astrocytes, we modified plasmid "pZac2.1final" (Penn Vector Core). We removed the *CMV* promoter flanked by *Bgl*II and *Hind*III sites and replaced it with the minimal (~700 bp) *GfaABC$_1$D* astrocyte-specific promoter, which was amplified by PCR from Addgene plasmid 19974. We then cloned Cre recombinase into this modified pZac2.1 vector between *Eco*RI and *Xba*I sites, to generate plasmids we called "pZac2.1 GfaABC$_1$D Cre". The fully sequenced "pZac2.1" plasmids were sent to the Penn Vector Core, which used them to generate AAV 2/5 for each construct at a concentration of ~2 x 10^{13} genome copies/ml (gc/ml). Our virus constructs have been deposited at Addgene in the Khakh lab repository (http://www.addgene.org/Baljit_Khakh). The AAVs are also available for purchase from the UPenn Vector Core (http://www.med.upenn.edu/gtp/vectorcore). The AAV2/5 GfaABC$_1$D Cre has recently been reported by us (Anderson et al., 2016). The AAV FLEX-GFP was originally made in the Sternson laboratory (Atasoy et al., 2008) and was purchased from the UPenn Vector Core.

Generation of *Aldh1l1*- and *Slc6A11*-Cre/ERT2 BAC transgenic mice

A 228 kb mouse BAC (RP23-7M9) containing the 48 kb mouse *Aldh1l1* coding region, a ~48 kb 5' flanking region and ~130 kb 3' flanking region was identified through a database search and obtained from the BACPAC Resource Center (Oakland Children's Hospital, Oakland, CA). Benefitting from an established protocol (Yang and Gong, 2005), the Cre/ERT2 cDNA (from Addgene plasmid #14797) was inserted into exon 1 of the *Aldh1l1* gene immediately preceding the translation initiation codon. Cloning steps for construction of the modified Aldh1l1 BAC targeting construct were essentially as described (Yang and Gong, 2005). Once completed, BAC purification, pronuclear injections and transgenic mouse generation was done at the University of California, Davis Mouse Biology Program (UC Davis MBP). Briefly, the modified Aldh1l1 BAC construct was purified and then injected into the pronucleus of fertilized oocytes. Injected oocytes were implanted into female FVB mice to generate pups. Founder pups were identified by PCR amplification of the Cre/ERT2 cassette. All founder pups were created in an FVB background and then backcrossed to C57/Bl6N mice till a 100% congenic C57/Bl6N strain expressing *Aldh1l1*-Cre/ERT2 was achieved. The *Aldh1l1*-Cre/ERT2 mice were backcrossed with C57/Bl6N mice for > 5 generations, i.e. to ~97% C57/Bl6N. The mice that are to be deposited at JAX have been backcrossed for 8 generations (i.e. to ~99% C57/Bl6N). Similar methods were used to generate *Slc6a11*-Cre/ERT2 BAC transgenic mice using BAC RP23-470B21 from the BACPAC Resource Center (Oakland Children's Hospital, Oakland, CA).

Generation of knock-in Lck-GCaMP6f^{flox} mice at the *ROSA26*

The Lck-GCaMP6f^{flox} mice contain a CMV-IE enhancer/chicken beta-actin/rabbit beta-globin hybrid promoter (CAG) promoter, followed by a loxP-3xSV40pA-loxP cassette, followed by the Lck-GCaMP6f cDNA at the *ROSA26* locus (Madisen et al., 2015). In brief, *ROSA26* targeting plasmid, called Ai39 was purchased from Addgene (plasmid #34884) and then modified to create the ROSA26 Lck-GCaMP6f targeting vector. Briefly, Lck-GCaMP6f was PCR amplified from the pZac2.1-GfaABC$_1$D-Lck-GCaMP6f plasmid and subcloned between *MluI* sites in the Ai39 plasmid to create the Lck-GCaMP6f *ROSA26* targeting plasmid. All cloning was performed using *Stbl2* cells (Invitrogen) that were propagated at 30°C in order to prevent recombination. Sequences of the targeting construct were confirmed with diagnostic restriction digests, PCR amplification and sequencing of the ampicillin and neomycin resistance cassette as well as the 5' and 3' homology arms. For electroporation of embryonic stem (ES) cells, the Lck-GCaMP6f *ROSA26* targeting plasmid was linearized with *Acl*I, which cuts at two sites within the ampicillin resistance cassette. Linearized plasmid DNA was precipitated overnight in 100% ethanol at 4°C. Following precipitation, DNA was sequentially washed in 70%, followed by 50% ethanol and then resuspended in TE buffer at a concentration of 720 μg/μl and a total volume of 150 μl. The linear plasmid was used to generate Lck-GCaMP6f knockin mice at UC Davis MBP. Briefly, the linearized *ROSA26* Lck-GCaMP6f construct was electroporated into C57BL/6 JM8.N4 ES cells and then selected with neomycin. 288 neomycin resistant clones were picked, cultured and expanded in 96-well plates. Drug resistant clones were subjected to genotype screening and confirmation testing for homologous recombination. ES cell clones were initially screened via a Loss-of-Allele (LOA) assay, which is a quantitative TaqMan PCR that detects the loss of one region of the native target due to correct recombination with the targeting vector. Thus, one observes a single copy of the native locus in the recombined ES cells and two copies of native loci in non-recombined ES cells. For loss of allele assays, ES cells

were processed in triplicate on an ABI7900HT quantitative PCR machine and analyzed via a relative cycle threshold method. Initial LOA candidates were expanded from the 96-well plate and then subjected to a selection cassette copy number analysis to ensure that there is only one copy of the neomycin resistance cassette. Both loxP sites in candidate ES cell recombinants were checked for DNA integrity. All recombinant ES cells candidates were also tested with long range PCR from vector/non genomic DNA to regions outside the long and short homology arms. Recombinant JM8N4 ES clones were injected into blastocysts and 30 embryos were implanted into two recipient mice per ES clone. Chimeric animals were scored based on coat color. Animals that showed >50% chimera were bred with WT mice to confirm germline transmission.

Other wild-type, transgenic and knock-in mice

B6;129S-*Gt(ROSA)26Sor*[tm95.1(CAG-GCaMP6f)Hze]/J (JAX# 024105), Tg(Slc1a3-cre/ERT)1Nat/J (JAX# 012586) and B6N.129-*Rpl22*[tm1.1Psam]/J (JAX# 011029) were acquired from the Jackson Laboratory. m*GFAP*-Cre 77.6 mice were available from past work (Gregorian et al., 2009). *Gjb6*-Cre/ERT2 mice were obtained from Dr. Frank Pfrieger (Institute of Cellular and Integrative Neurosciences, Strasbourg France). Transgenic and knock-in mice were maintained by breeding with C57BL6/N mice (from Taconic), and hemizygous transgenic mice were used for experiments. All the mice were housed with food and water available *ad libitum* in a light controlled environment. Both male and female mice at 10 weeks' old were used for experiments.

Generation of Ai95 x *Aldh1l1*-Cre/ERT2 and Lck-GCaMP6f x *Aldh1l1*-Cre/ERT2 double transgenic mice

To generate double transgenic mice, heterozygous Ai95 or Lck-GCaMP6f[flox] mice were crossed with hemizygous *Aldh1l1*-Cre/ERT2 BAC mice. The Ai95 and Lck-GCaMP6f[flox] knock-in mice respectively possess a floxed knock-in of cyto-GCaMP6f and Lck-GCaMP6f in the ROSA26 locus, while *Aldh1l1*-Cre/ERT2 BAC mice possesses promoter and enhancer elements of the *Aldh1l1* gene driving expression of Cre/ERT2. Double transgenic pups were identified by genotyping for GCaMP6f at the *ROSA26* locus (forward primer 5'–AGCTCGCCTACCACTACCAGCA–3'; reverse primer 5'–TTGAAGAAGATGGTGCGCTCCTG–3') and Cre/ERT2 (forward primer 5'– AGACCAATCATCAGGATCTCTAGCC–3'; reverse primer 5'–CATGCAAGCTGGTGGCTGG–3') in two separate PCR reactions for each pup. Double transgenic progeny used for experiments are heterozygous for either cyto-GCaMP6f or Lck-GCaMP6f at the *ROSA26* locus and hemizygous for the *Aldh1l1*-Cre/ERT2 insert.

Stereotaxic AAV microinjections into the hippocampus

Stereotaxic injections into the mouse hippocampus were done as previously described (Shigetomi et al., 2013). Mice at ~P56 were used in all experiments in accordance with institutional guidelines. All surgical procedures were conducted under general anesthesia using continuous isoflurane (induction at 5%, maintenance at 1–2.5%, vol/vol). Depth of anesthesia was monitored continuously and adjusted when necessary. Following induction of anesthesia, the mice were fitted into a stereotaxic frame with their heads secured by blunt ear bars and their noses placed into an anesthesia and ventilation system (David Kopf Instruments). Mice were administered 0.05 ml of buprenorphine (Buprenex, 0.1 mg ml^{-1}) subcutaneously before surgery. The surgical incision site was then cleaned three times with 10% povidone iodine and 70% ethanol (vol/vol). Skin incisions were made, followed by craniotomies of 2–3 mm in diameter above the left parietal cortex using a small steel burr (Fine Science Tools) powered by a high-speed drill (K.1070, Foredom). Saline (0.9%) was applied onto the skull to reduce heating caused by drilling. Unilateral viral injections were carried out by using a stereotaxic apparatus (David Kopf Instruments) to guide the placement of beveled glass pipettes (1B100-4, World Precision Instruments) into the left hippocampus. The coordinates were 2 mm posterior to bregma, 1.5 mm lateral to midline, and 1.6 mm from the pial surface. 1 μl of AAV2/5 CAG-FLEX-GFP virus at ~10^{13} genome copies per ml was injected by using a syringe pump (Pump11 PicoPlus Elite, Harvard Apparatus). Glass pipettes were left in place for at least 10 min. Surgical wounds were closed with single external 5-0 nylon sutures. Following surgery, animals were allowed to recover overnight in cages placed partially on a low-voltage heating pad. Buprenorphine was administered two times per day for up to 2 d after surgery. In addition, trimethoprim sulfamethoxazole in food was provided to the mice for 1 week. AAV2/5 CAG-FLEX-GFP injected mice were perfused 2 weeks after the last tamoxifen injection for immunohistochemistry, while AAV2/5 GfaABC$_1$D-Cre (Anderson et al., 2016) injected mice were euthanized two weeks post-surgery for live slice imaging and immunohistochemistry (typically 13–15 d).

Tamoxifen administration to adult mice

Tamoxifen (Sigma) was freshly prepared at a concentration of 20 mg/ml in corn oil and dissolved overnight with continuous agitation. To induce gene expression, tamoxifen was administered intraperitoneally in a volume of

100 µl per mouse for five consecutive days, using a 1 ml syringe and a 25 G 5/8-inch needle (BD Biosciences). Experiments were performed two weeks after the last tamoxifen injection.

Head bar installation and cranial window surgery

Five days after tamoxifen injections (see above), adult (> 8 weeks) male and female mice of the relevant genotypes were anesthetized with isoflurane and placed in a stereotaxic frame (Kopf). Dexamethasone (0.2 mg/kg) was administrated subcutaneously before surgery began. Surgery was performed under standard and sterile conditions. After hair removal and lidocaine application (2%, Akorn), the mouse's skull was exposed from the frontal to the intraparietal bone, and the connective tissue was carefully removed from the skull for the custom-made head bar to be glued on using cyanoacrylate (Krazy Glue). Vetbond (3M) was used to close the incision site. A small chamber then was made surrounding the incision site with black dental cement (Ortho-Jet, Lang Dental) to hold water for water-immersion objective lens during imaging. A 3 mm diameter circular craniotomy was performed carefully using a dental drill bit with the center located at 2.5 mm lateral to lambda (**Figure 5A**). The cranial window was then sealed with a 3 mm diameter round #1 coverslip using Vetbond. The animal was given carprofen (5 mg/kg) and amoxicillin (BIOMOX, Virbac Animal Health) post-surgery for at least a week to recover from the surgery before subjecting to imaging.

***In vivo* two-photon laser scanning microscopy (2PLSM) and air puff startle**

Two-photon laser-scanning microscopy was performed with a Moveable Objective Microscope (Sutter MOM) using a Ti-Sapphire laser (Coherent Ultra II) at 920 nm, through a 40X 0.8 NA water-immersion objective (Olympus). The objective was mounted at a tilt of 30 degrees to the vertical axis in order to image with the light path perpendicular to the cranial window and the cortical surface. Images were acquired using the *ScanImage* software (Vidrio Technologies) and processed with *ImageJ* (NIH). Fully awake mice, without any anesthesia, were mounted on top of a spherical treadmill by securing its head-bar onto a custom-made head-bar holder under the microscope. The treadmill consisted of an 8-inch diameter Styrofoam ball resting inside another Styrofoam hollow half-sphere (Graham Sweet Studios) into which a constant stream of compressed air was blown to keep the ball afloat, allowing mice to freely run or rest on top. Images were acquired every 750 ms (1.33 Hz). To track the mouse's locomotion, the treadmill motion was measured every 25 ms (40 Hz) by a custom-designed optical sensor whose signals were converted into two servo pulse analog signals (front-back and left-right) using an external PIC microcontroller. The locomotion data were acquired simultaneously with the calcium imaging data and synchronized through the scanning mirror signals. These analog signals were digitized with a NIDAQ board (National Instruments) and acquired with the WinEDR software (Strathclyde). The microscope and treadmill were encased in a light-tight box, and the animals were kept in darkness without visible visual stimuli during the imaging sessions. Before experiments, mice were acclimated to the head fixation and to resting and running on the spherical treadmill, as previously described (Polack et al., 2013; Srinivasan et al., 2015).

Startle was induced by presenting a brief air puff to the face of the mice while the mice were resting on top of the spherical treadmill during the imaging sessions. The air puff was delivered by pressing a hand-pump air compressor (28 x 5 cm) attached to a ¼-inch PVC tubing with its opening positioned ~1 cm away from the nostril of the mice (**Figure 5A**). One press of the hand pump generated a ~3 s long gentle air puff. Behavioral startle was confirmed by the locomotion induced immediately after presenting the air puff.

Immunohistochemical (IHC) evaluations

For transcardial perfusion, mice were euthanized with pentobarbitol (i.p.). Once all reflexes subsided the abdominal cavity was opened and heparin (0.1 ml) was injected into the heart to prevent the blood from clotting. The animal was perfused with 50 ml ice cold 0.1 M phosphate buffered saline (PBS) followed by 50 ml 10% buffered formalin (Fisher). After gentle removal from the skull, the brain was post fixed in 10% buffered formalin overnight. The tissue was cryoprotected in buffered 30% sucrose solution the following day for at least 2 days at 4°C until use. 40 µm coronal frozen sections were prepared using a cryostat microtome (Leica) and processed for immunohistochemistry. To stain cyto-GCaMP6f and Lck-GCaMP6f for brightfield microscopy, sections were washed in 0.1 M tris buffered saline (TBS) and treated with 1% H_2O_2 for 20 min to block endogenous peroxidase activity. The sections were incubated with 10% normal goat serum (NGS) and 0.5% Trition-X 100 in 0.1 M TBS at room temperature for 60 min. Sections were then incubated with a chicken anti-GFP antibody (1:1000; Abcam Cat# ab13970 RRID:AB_300798) in 0.1 M TBS overnight at 4°C. After three 10 min washes in 0.1 M TBS, followed by incubation with biotinylated goat anti-chicken antibody (1:400; Vector ABC Standard kit) in 0.1 M TBS with 10% NGS for 1 hr at room temperature. After another three 10 min washes in 0.1 M TBS, the sections were incubated for 1 hr at room temperature in an avidin–biotin complex, which was made by mixing one drop each of A and B

solutions from the Vector ABC Standard Kit. Staining was visualized by incubation with a mixture of developing buffer from the ABC Standard Kit, diaminobenzidine (DAB, Sigma) as the developing agent and H_2O_2 in ddH2O, which causes dark brown staining in areas with cyto-GCaMP6f or Lck-GCaMP6f expression. Brain sections were subsequently dehydrated and mounted with Eukitt (Calibrated Instruments).

To immunostain for fluorescence microscopy, 40 μm coronal sections were washed 3 times in 0.1 M PBS for 10 min each, and then incubated in a blocking solution containing 10% NGS in 0.1 M PBS with 0.5% Triton-X 100 for 1 hr at room temperature with agitation. Sections were then incubated in primary antibodies diluted in 0.1 M PBS with 0.5% Triton-X 100 overnight at 4°C. The following primary antibodies were used: chicken anti-GFP (1:1000; Abcam Cat# ab13970 RRID:AB_300798), mouse anti-NeuN (1:1000; Abcam Cat# ab104225 RRID:AB_10711153), Rabbit anti-NeuN (1:1000; Cell Signaling; RRID: AB_2630395), Mouse anti-HA (1:1000; Covance; RRID: AB_291230) chicken anti-GFAP (1:1000, Abcam Cat# ab4674 RRID:AB_304558), guinea pig anti-Glt1 (1:1000, Millipore Cat# AB1783 RRID:AB_90949) and rabbit anti S100β (1:1000, Abcam Cat# ab41548 RRID:AB_956280). The next day the sections were washed 3 times in 0.1 M PBS for 10 min each before incubation at room temperature for 1 hr with secondary antibodies diluted in 0.1 M PBS. The following Alexa conjugated secondary antibodies were used: goat anti-chicken 488 (1:1000, Molecular Probes Cat# A-11039 RRID:AB_142924), goat anti-rabbit 546 (1:1000, Molecular Probes Cat# A-11035 RRID:AB_143051), goat anti-chicken 647 (1:1000, Thermo Fisher Scientific Cat# A-21449 RRID:AB_2535866), goat anti-guinea pig 546 (1:1000, Thermo Fisher Scientific Cat# A-11074 RRID:AB_2534118) and goat anti-mouse 546 (1:1000, Molecular Probes Cat# A-11030 RRID:AB_144695). The sections were then rinsed 3 times in 0.1 M PBS for 10 min each before being mounted on microscope slides. Fluorescence images were taken using UplanSApo 20X 0.85 NA and UPlanFL 40X 1.30 NA oil immersion objective lens and the FV300 Fluoview confocal laser-scanning microscope. We used the 488 nm line of an Argon laser to excite Alexa488, with the intensity adjusted to 0.5–5% of the maximum output, which was 10 mW. The emitted light pathway consisted of an emission high pass filter (505-525 nm) before the photomultiplier tube. Alexa 546 and Alexa 594 were excited by the 543 nm laser line of the HeNeG laser at 30% of the maximum output (1 mW). The emitted light pathway consisted of a dichroic mirror (SDM560) and a 560–600 nm emission filter. The data shown in Supp Movie 1 were gathered using an automated Nikon C2 confocal microscope and a 20X oil immersion lens.

Astrocyte calcium imaging with confocal microscopy in acute brain slices

Coronal slices of hippocampus (300 μm) were cut in solution comprising (mM): 87 NaCl, 25 NaHCO₃, 2.5 KCl, 1.25 NaH₂PO₄, 25 D-glucose, 75 sucrose, 7 MgCl₂ and 0.5 CaCl₂, saturated with 95% O₂ and 5% CO₂. Slices were incubated at ~34 °C for 30 min and subsequently stored at 21–23 °C in artificial cerebrospinal fluid (aCSF) comprising (mM): 126 NaCl, 2.5 KCl, 1.3 MgCl₂, 10 D-glucose, 2.4 CaCl₂, 1.24 NaH₂PO₄, and 26 NaHCO₃, saturated with 95% O₂ and 5% CO₂. All other slice procedures were exactly as described previously (Shigetomi et al., 2013). All imaging was performed using a commercially available off-the-shelf and standard confocal microscope. In brief, cells for a majority of the experiments were imaged using a confocal microscope (Fluoview 1000; Olympus) with a 40X water-immersion objective lens with a numerical aperture (NA) of 0.8 and at a digital zoom of three. Hippocampal ATP responses were acquired with a 0.3 NA, 10X water-immersion lens and at 1X digital zoom. We used the 488 nm line of an Argon laser, with the intensity adjusted to 0.5–5% of the maximum output of 10 mW. The emitted light pathway consisted of an emission high pass filter (>510 nm) before the photomultiplier tube. Astrocytes were selected from the visual cortex, layer II/III and were typically ~40 μm below the slice surface and scanned at 1 frame per second for 600 s.

Adult cortical astrocyte transcriptome evaluations

RNA was collected from cortices of *Aldh1l1*-cre/ERT2 x RiboTag mice (RRID: IMSR_JAX:011029) based on a published protocol (Sanz et al., 2009). Briefly, freshly dissected cortices were collected from four animals (P78 - P82), 3 males and 1 female, and homogenized. RNA was extracted from 15% of cleared lysate as input. The remaining lysate was incubated with mouse anti-HA antibody (Covance #MMS-101R RRID: AB_291263) with rocking for 4 hours at 4°C followed by addition of magnetic beads (Invitrogen Dynabeads #100.04D) and overnight incubation with rocking at 4°C. The beads were washed three times in high salt solution. The bound ribosomes and RNA were separated from the beads with 30 s of vortexing in RLT lysis buffer as IP. RNA was purified from the IP and corresponding input samples (Qiagen RNeasy Plus Micro #74034). RNA concentration and quality were assessed with nanodrop and Agilent 2100 Bioanalyzer. RNA samples with RNA integrity number (RIN) greater than nine were used for multiplexed library prep with KAPA Stranded RNA-Seq Kit with mRNA enrichment (#KK8401). Sequencing was performed on Illumina NextSeq 500 for 2x75. Data quality check was done on Illumina SAV. Demultiplexing was performed with Illumina Bcl2fastq2 v 2.17 program. Reads were aligned to the

16

latest mouse mm10 reference genome using the STAR spliced read aligner (~84% reads mapped uniquely). Fragment counts were derived using HTS-seq program. Differentially expressed genes were identified using bioconductor packages and Limma-Voom with adjustment for difference between animals, which are then considered and ranked based on adjusted P-values (FDR) of < 0.05.

To determine the P80 astrocyte enriched genes, the IP enriched gene list at FDR < 0.05 was filtered for enrichment fold change (FC) > 2 versus input. Genes that had FPKM values of 0 for either input or IP were also filtered out to exclude genes with exaggerated FC values. The P7 astrocyte-enriched genes were determined with FC > 2 for astrocyte FPKM versus average FPKM of all cell types. Transcripts that were enriched at P80 and/or P7 constituted the master list of 4727 astrocyte enriched transcripts used to look for developmental changes in gene expression. To compare P80 and P7 datasets, transcript expression was normalized as percentile of highest FPKM transcript (percentile FPKM; from 0 to 1) in IP and Zhang *et al*. astrocyte samples, respectively. *Apoe* (P80 highest) and *Fos* (P7 highest) were both in the list of 4727 astrocyte enriched transcripts. The Rank-rank Hypergeometric Overlap algorithm (Plaisier et al., 2010) was used to assess similarity between datasets. We focused on transcripts with a change in percentile (delta percentile) of at least 0.1 to highlight transcripts with different expression between P90 and P7 datasets.

Raw and normalized RNAseq data have been deposited in the Gene Expression Omnibus repository (http://www.ncbi.nlm.nih.gov/geo) with accession number GSE84540.

Chemicals

All chemicals used were from VWR, Tocris, Alomone or Sigma. In the text, the names of the chemicals abbreviated are adenosine 5' triphosphate (ATP), phenylephrine (PE), tetrodotoxin (TTX).

Supplemental references

Anderson, M.A., Burda, J.E., Ren, Y., Ao, Y., O'Shea, T.M., Kawaguchi, R., Coppola, G., Khakh, B.S., Deming, T.J., and Sofroniew, M.V. (2016). Astrocyte scar formation aids central nervous system axon regeneration. Nature *532*, 195-200.

Atasoy, D., Aponte, Y., Su, H.H., and Sternson, S.M. (2008). A FLEX switch targets Channelrhodopsin-2 to multiple cell types for imaging and long-range circuit mapping. J Neurosci *28*, 7025-7030.

Chow, L.M., Zhang, J., and Baker, S.J. (2008). Inducible Cre recombinase activity in mouse mature astrocytes and adult neural precursor cells. Transgenic Res *17*, 919-928.

Gregorian, C., Nakashima, J., Le Belle, J., Ohab, J., Kim, R., Liu, A., Smith, K.B., Groszer, M., Garcia, A.D., Sofroniew, M.V.*, et al.* (2009). Pten deletion in adult neural stem/progenitor cells enhances constitutive neurogenesis. J Neurosci *29*, 1874-1886.

Madisen, L., Garner, A.R., Shimaoka, D., Chuong, A.S., Klapoetke, N.C., Li, L., van der Bourg, A., Niino, Y., Egolf, L., Monetti, C.*, et al.* (2015). Transgenic mice for intersectional targeting of neural sensors and effectors with high specificity and performance. Neuron *85*, 942-958.

Madisen, L., Zwingman, T.A., Sunkin, S.M., Oh, S.W., Zariwala, H.A., Gu, H., Ng, L.L., Palmiter, R.D., Hawrylycz, M.J., Jones, A.R.*, et al.* (2010). A robust and high-throughput Cre reporting and characterization system for the whole mouse brain. Nat Neurosci *13*, 133-140.

Nakamura, E., Nguyen, M.T., and Mackem, S. (2006). Kinetics of tamoxifen-regulated Cre activity in mice using a cartilage-specific CreER(T) to assay temporal activity windows along the proximodistal limb skeleton. Dev Dyn *235*, 2603-2612.

Plaisier, S.B., Taschereau, R., Wong, J.A., and Graeber, T.G. (2010). Rank-rank hypergeometric overlap: identification of statistically significant overlap between gene-expression signatures. Nucleic Acids Res *Sep;38(17):e169. doi: 10.1093/nar/gkq636. Epub 2010 Jul 21.*

Polack, P.O., Friedman, J., and Golshani, P. (2013). Cellular mechanisms of brain state-dependent gain modulation in visual cortex. Nat Neurosci *16*, 1331-1339.

Sanz, E., Yang, L., Su, T., Morris, D.R., McKnight, G.S., and Amieux, P.S. (2009). Cell-type-specific isolation of ribosome-associated mRNA from complex tissues. Proc Natl Acad Sci U S A *106*, 13939-13944.

Shigetomi, E., Bushong, E.A., Haustein, M.D., Tong, X., Jackson-Weaver, O., Kracun, S., Xu, J., Sofroniew, M.V., Ellisman, M.H., and Khakh, B.S. (2013). Imaging calcium microdomains within entire astrocyte territories and endfeet with GCaMPs expressed using adeno-associated viruses. J Gen Physiol *141*, 633-647.

Srinivasan, R., Huang, B.S., Venugopal, S., Johnston, A.D., Chai, H., Zeng, H., Golshani, P., and Khakh, B.S. (2015). Ca(2+) signaling in astrocytes from Ip3r2(-/-) mice in brain slices and during startle responses in vivo. Nat Neurosci *18*, 708-717.

Yang, X.W., and Gong, S. (2005). An overview on the generation of BAC transgenic mice for neuroscience research. Curr Protoc Neurosci *May;Chapter 5:Unit 5.20*.